International Journal of Modern Manufacturing Technologies
ISSN 2067–3604, Vol. XIV, No. 2 / 2022
https://doi.org/ 10.54684/ijmmt.2022.14.2.208

CORROSION PREVENTION ON S45C USING HARDENING METHOD

Muhammad Akhlis Rizza, Ratna Monasari, Zakki Fuadi Emzain, Asrori Asrori, Ilham Krissetyawan Nusantara

State Polytechnic of Malang-Indonesia, Department of Mechanical Engineering
Jl. Sukarno Hatta no 9 Malang 65144 Indonesia

Corresponding author: Muhammad Akhlis Rizza, muh.akhlis@polinema.ac.id

Abstract: This study aims to determine the effect of holding time and oil viscosity on the S45C steel hardening process on the corrosion rate. The corrosion rate is measured using the weight loss method. Micro-photo observations of the S45C steel surface were carried out to determine the type of corrosion. The results demonstrate that the corrosion rate of hardened S45C steel decreases following the longer holding time during hardening. In addition, the corrosion rate of hardened S45C steel decreases when the viscosity of the oil used during hardening is thicker. Finally, the type of corrosion is uniform and pitting corrosion.
Keywords: holding time, oil viscosity, hardening, S45C steel, corrosion rate.

1. INTRODUCTION

A key component of contemporary technology is materials technology. The characteristics of materials and our understanding of them frequently place limits on technological advancement. Some characteristics, like those that affect corrosion behavior, are particularly challenging to identify and manage. According to estimates, the cost of corrosion in industrialized nations ranges from 3 to 4% of GDP. Furthermore, it has been calculated that a better application of current knowledge in corrosion prevention, design, and so forth, may have prevented roughly 20% of this loss. In other words, there is a need for technical advancement, applied research, education, information, and transfer of knowledge and technology (Bardal, 2004).

Pumps have been widely used in almost all industrial fields, such as in cooling, heating, lubrication, hydraulic processes, and water transportation. In its use, however, it is crucial to pay attention to the pumping system as it uses up to 25-50% of energy in an industry (Cardoso et al., 2017).

During the pumping operation, the pump shaft is constantly degraded by corrosion or mechanical degradation. The pump shaft is generally exposed to the fluid that is continuously pumped along the tunnel. The pump has been installed with safety tools such as rings or seals in other forms. However, leaks are still common to happen, and this is raising the risk of corrosion (Berndt & van Bennekom, 2001). Two major components of a pump that have the highest risk for corrosion are the shaft and the tube (Vazdirvanidis et al., 2017).

Corrosion is one of the most common examples of pump shaft damage that degrades its performance in a seawater working environment. The shaft is damaged by corrosion due to environmental factors, stresses, and the microstructure of the material (Clover et al., 2005; Li & Akid, 2013).

Prior studies concluded that corrosion, especially in aqueous environments, is caused by potential differences on very narrow surfaces due to material heterogeneity. This material heterogeneity ranges in atomic size up to several microns and can result from defects in the crystal structure, chemical phase differences, element segregation, or non-metallic inclusions. Generally, heterogeneity is influenced by the composition, as well as the mechanical and thermal treatment of the material (Clover et al., 2005).

Variations in composition and heat treatment that occur in the material significantly affect corrosion resistance. Heat treatment of carbon, manganese, phosphorus, and sulfur also affects corrosion resistance. Generally, alloy composition, warmness remedy, and mechanical processing affect the transformation behavior of many sections, mechanical properties, corrosion resistance, and processing (Hwang & Park, 2009).

Research on AISI 410 Stainless Steel material demonstrates that its corrosion properties are related to the number and size of carbides, impurities, grain boundaries, and microstructure (Moradi et al., 2019). Preheating the surface was shown to increase surface hardness and improve corrosion resistance.

Preheating was also carried out on AISI P20 steel material. AISI P20 steel is commonly used for molding. One of the results of heating treatment is the

increase in anti-corrosion properties (Z. Li et al., 2020).
In another study, the heating of chromium stainless steel 9M340, N695, and Corrax is done to improve the anti-corrosion properties. Interestingly, it is reported that anti-corrosion properties are improved, especially with CuSO4 corrodents (Brühl et al., 2010).
Many researchers have been studying heating as a method to improve corrosion resistance. However, there is no empirical report regarding S45C material so far even though S45C is widely used as a shaft in pumps which also has a high risk of corrosion.
The objective of this study is to investigate the significance of heat treatment in improving the corrosion resistance S45C properties.

2. MATERIALS AND METHODS

Initially, S45C steel is hardened at 850℃ with varying holding times of 30, 60, and 90 minutes. Oil with various viscosities SAE 0W-20, SAE 5W-30, and SAE 20W-50 are used as the coolant. The testing of corrosion rate is conducted using the weight loss method. Furthermore, S45C steel specimens are immersed in 32% HCl solution for 168 hours. Finally, the surface of S45C steel specimens is observed with micro photography to determine the type of corrosion that occurred.

2.1 Material

The materials used in this study include S45C steel with 25 mm diameter, HCl solution (32%), acetone, distilled water, oil with various viscosities; SAE 0W-20, SAE 5W-30, and SAE 20W-50 that are used for cooling medium during the hardening process. S45C steel (JIS G 4051) is a type of medium carbon steel with a chemical composition of C (0.46%), Mn (0.54%), Si (0.21%), S (0.006%), P (0.023%), Ni (0.01%), Cr (0.36%), and Cu (0.02%).

2.2 Specimen Manufacturing Process

S45C steel is obtained from a metal shop in the form of a 1-inch diameter workpiece, which is then transformed into 24 mm. The next preparation stage is cutting the steel with a cutting grinder to produce a 10 mm thick steel. The surface of the specimen is smoothed using a rotating grinding machine.

2.3 Hardening

The holding times that are applied in the hardening process are 30, 60, and 90 minutes. In sequence, the hardening process is carried out in exact order. The first process is the installation of wire as a mounting on the specimen to facilitate the process of removing the specimen from the metal furnace (1). Then, specimens are inserted according to code (2). The next process is the application of the heating treatment with a temperature of 850 ℃ (3). The holding time is then started when the temperature has reached 850 ℃ (4). The holding time for each specimen is 30, 60, and 90 minutes, respectively. After reaching the predetermined holding time, the next process is dipping the specimen into the oil with varying viscosity; SAE 0W-20, SAE 5W-30, and SAE 20W-50 (5). Finally, the last process is cleaning the specimens to remove scale and oil (6). Wire mesh and acetone are used for cleaning the specimens. The specimens are prepared for micro photo observation.

2.4 Corrosion Rate Testing

The testing of corrosion rate refers to ASTM G31-72, as explained in "Standard Practice for Laboratory Immersion Corrosion Testing of Metal" (Jannifar et al., 2019). The corrosion medium used in the corrosion test is 32% HCl solution and the immersion time of the specimen is 168 hours.
The test begins with weighing the hardened specimens using analytical scales. Then, the specimens are arranged in a plastic container containing 32% HCL - according to the viscosity of the oil used as a cooling medium. The use of HCl solution is 0.2 ml per mm2 of the surface area of each specimen. The specimens are immersed for 168 hours and then pickled with acetone and distilled water. Finally, specimens are prepared for final weighting using an analytical balance.
The corrosion rate is calculated using the following formula (Davis, 2000):

$$\text{Corrosion Rate} = \frac{K \times W}{A \times T \times D} \quad (1)$$

Note: K: Constanta ($8{,}76 \times 10^4$), T: Immersion Time (hour), A: Surface Areas (cm^2), W: Lost Mass (g), D: Density (g/cm^3)

2.5 Micro-photo Observation

The micro photo observation of the S45C surface is important for studying the type of corrosion that occurred after the treatment. Micro photo observations are conducted using a digital microscope with 800x magnification.

3. RESULT AND DISCUSSION

After conducting corrosion testing for 168 hours in 32% HCl solution, the data on the corrosion rate of S45C steel is shown in Table 1.

Table 1. Corrosion Rate

Holding time (minute)	Oil Type	Specimen Code	Corrosion Rate (mm/y)	Average (mm/y)
30	SAE 0W-20	A1; A2; A3	79,0; 82,3; 79,9	80.4
30	SAE 5W-30	A4; A5; A6	76,1; 76,9; 76,3	76.5

30	SAE 20W-50	A7; A8; A9	76,3; 77,3; 75,1	76.2
60	SAE 0W-20	B1; B2; B3	84,0; 83,5; 82,1	83.2
60	SAE 5W-30	B4; B5; B6	83,3; 80,8; 83,0	82.4
60	SAE 20W-50	B7; B8; B9	74,4; 76,3; 75,4	75.4
90	SAE 0W-20	C1; C2; C3	82,1; 83,2; 81,5	82.3
90	SAE 5W-30	C4; C5; C6	77,7; 77,9; 80,2	78.6
90	SAE 20W-50	C7; C8; C9	74,8; 74,0; 77,8	75.5

Furthermore, the descriptive comparison of corrosion rates is explained in figure 1.

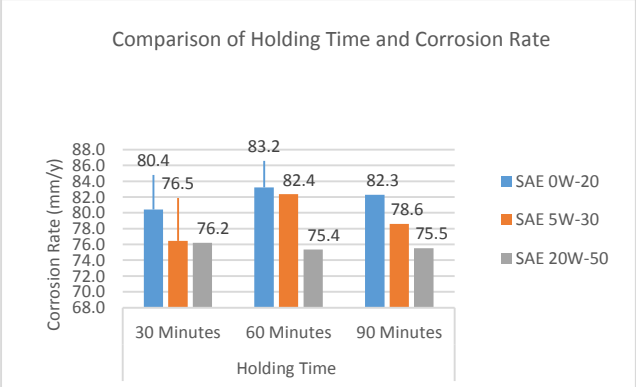

Fig. 1. Descriptive comparison between holding time and corrosion rate

Based on Figure 1, the highest average corrosion rate is 82.4 mm/y at a holding time of 60 minutes. On the other hand, the lowest average is 75.4 mm/y at a holding time of 60 minutes. Furthermore, the graph also demonstrates a downward trend in the average corrosion rate as the holding time increases. This is because the temperature is getting thoroughly absorbed from the surface to the core of S45C following the longer heat exposure. Therefore, the structure of S45C steel changes into the austenite phase homogeneously. In addition, during the quenching process, S45C steel in the austenite phase can transform into a martensite structure evenly as the length of the holding time increases (Carlone et al., 2010). The effect of oil viscosity on corrosion rate is explained in Figure 2.

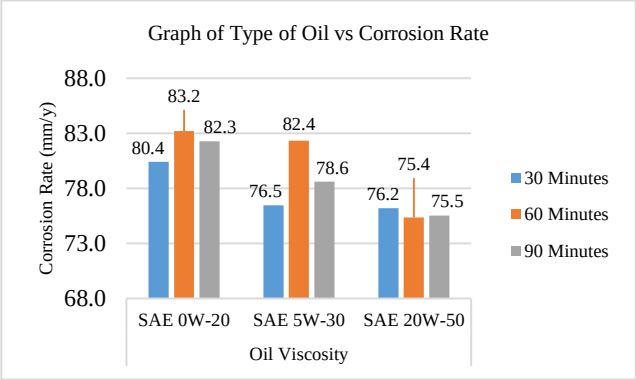

Fig. 2. Descriptive comparison between oil and corrosion rate

Figure 2 demonstrates that the highest average corrosion rate occurred in the dipping of 82.4 mm/y oil with SAE 0W-20 viscosity. Meanwhile, the lowest average corrosion rate is 75.4 mm/y, dipped in SAE 20W-50 viscosity oil during the cooling process. The graph also demonstrates a decrease in the corrosion rate as the oil viscosity value increases during the cooling process. The higher the oil viscosity, the slower the cooling process of the S45C. In addition, the formation of martensite structure is also becoming more difficult. Therefore, S45C steel has mechanical properties that tend to be soft and ductile as the oil viscosity value increases (Wu et al, 2014).

Micro photo observation on the surface of S45C steel is important to determine the type of corrosion that occurred after testing for 168 hours. Table 3 displays the results of micro photo observations of the surface of S45C specimens.

Table. 3 Results of micro photo observation

Micro photo of specimen	Remark
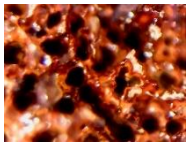	Holding time: 30 minutes Type of oil: SAE 0W-20 Micro-photo of the top view demonstrates uniform corrosion. Large holes are evenly distributed.
	Holding time: 30 minutes Type of oil: SAE 0W-20 The side view shows uniform corrosion with evenly distributed grooves.
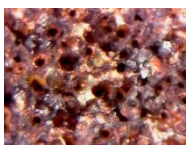	Holding time: 30 minutes Type of oil: SAE 0W-20 The bottom view shows uniform corrosion with evenly spread small holes.
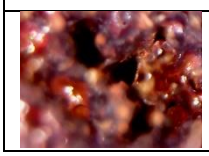	Holding time: 30 minutes Type of oil: SAE 5W-30 The top view shows uniform corrosion with large holes.

Micro photo of specimen	Remark
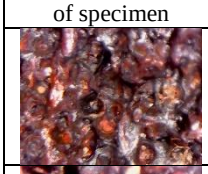	Holding time: 30 minutes Type of oil: SAE 5W-30 The side view shows uniform corrosion.
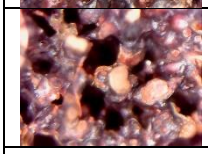	Holding time: 30 minutes Type of oil: SAE 5W-30 The bottom view shows large holes that are evenly distributed.
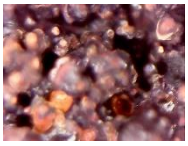	Holding time: 30 minutes Type of oil: SAE 20W-50 The top view shows uniform corrosion where the pores have varying sizes and are evenly spread.
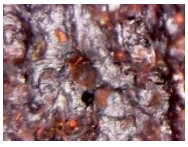	Holding time: 30 minutes Type of oil: SAE 20W-50 The side view shows uniform corrosion despite an uneven surface. The pores are rather small.
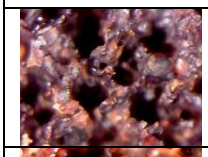	Holding time: 30 minutes Type of oil: SAE 20W-50 The bottom view shows uniform corrosion with large holes.
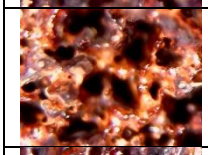	Holding time: 60 minutes Type of oil: SAE 0W-20 The top view shows uniform corrosion with large holes.
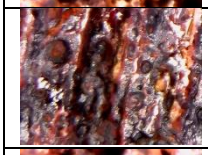	Holding time: 60 minutes Type of oil: SAE 0W-20 The side view shows uniform corrosion with evenly distributed grooves.
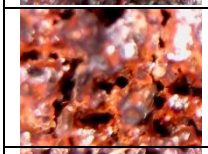	Holding time: 60 minutes Type of oil: SAE 0W-20 The bottom view shows uniform corrosion. Pores have various sizes.
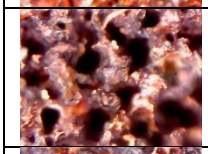	Holding time: 60 minutes Type of oil: SAE 5W-30 The top view shows uniform corrosion with evenly distributed large holes.
	Holding time: 60 minutes Type of oil: SAE 5W-30 The side view shows corrosion with evenly distributed small grooves.
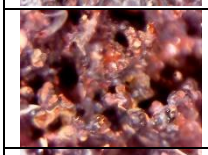	Holding time: 60 minutes Type of oil: SAE 5W-30 The bottom view shows even corrosion with various hole sizes.
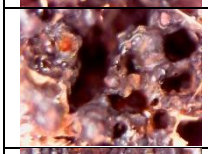	Holding time: 60 minutes Type of oil: SAE 20W-50 The top view shows corrosion with evenly distributed large holes.
	Holding time: 60 minutes Type of oil: SAE 20W-50 The side view shows uniform corrosion. Grooves have varying sizes.

Micro photo of specimen	Remark
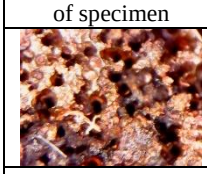	Holding time: 60 minutes Type of oil: SAE 20W-50 The bottom view shows even corrosion with evenly distributed small holes.
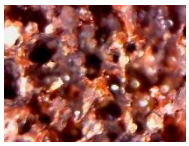	Holding time: 90 minutes Type of oil: SAE 0W-20 The top view shows even corrosion. Holes have varying sizes and are evenly distributed
	Holding time: 90 minutes Type of oil: SAE 0W-20 The side view shows corrosion with evenly distributed grooves.
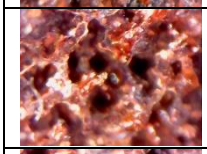	Holding time: 90 minutes Type of oil: SAE 0W-20 The bottom view shows uniform corrosion with large holes
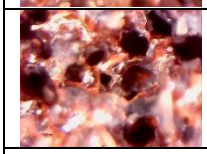	Holding time: 90 minutes Type of oil: SAE 5W-30 The top view shows even corrosion with several large holes.
	Holding time: 90 minutes Type of oil: SAE 5W-30 The side view shows uniform corrosion despite an uneven surface. Holes have a large size.
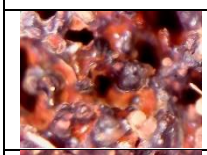	Holding time: 90 minutes Type of oil: SAE 5W-30 The bottom view shows uniform corrosion. Pores have various sizes.
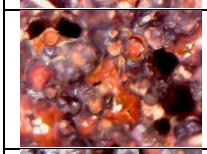	Holding time: 90 minutes Type of oil: SAE 20W-50 The top view shows uniform corrosion with several large holes.
	Holding time: 90 minutes Type of oil: SAE 20W-50 The side view shows evenly spread grooves.
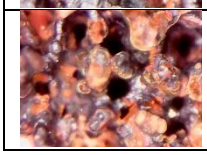	Holding time: 90 minutes Type of oil: SAE 20W-50 The bottom view shows uniform corrosion with large holes.

Based on Figure 3, it is confirmed that most specimens experience uniform corrosion with various holes on every surface area. Other than that, few specimens express pitting corrosion (Davis, 2000).

For simplicity, the basic pit process can be divided into three stages. The first stage is the germination of the seeds which leads to the formation of a small area of the bare and unmovable passive metal surface. The second phase is the development of a metastable fossa which leads to the local melting of a significant portion

of the underlying metal. The dissolved metal region is called the pit embryo. The result is the formation of a stable pit or repassivation. Finally, the third stage is the growth of a stable well which leads to the metal damage and propagation of the pit (Jirarungsatian & Prateepasen, 2010).

The cause of pitting corrosion is due to the penetration of 32% HCl solution on the surface of the specimen caused by gravity. The penetration causes the formation of pits and grooves on the surface of the S45C steel (Yim et al., 2007).

Generally, pitting is started in passive materials at first, such as aluminum and stainless steel, by the adsorption of halide ions that pierce the passive coating at specific locations. This occurs in weak spots in the oxide film, such as abnormalities caused by metal inclusions or grain boundaries in the oxide structure. The oxide layer's ion conductivity increases significantly due to the absorption of halide ions, allowing metal ions to move through the film. This causes localized dissolution, which leads to the formation of intrusions in the metal surface (Bardal, 2004).

Pitting corrosion, sometimes referred to as pinhole corrosion, is a very limited form of pinhole corrosion that affects a specific area of stainless steel. The pitting acts as the anode for the micro-corrosion cell, which is created surrounding the pitting and is known as the "small anode, large cathode" region, as a result of the local surface of passive film being broken down in the Cl- contained sensitive environment. Within pitting, there are anode reactions $M \rightarrow M^{n+}+ne-$.

Outside of pitting, there is also the cathode reaction concurrently:$1/2\ O_2 + H_2O + 2e- \rightarrow 2OH-$. To prevent dissolved oxygen from diffusing into pitting and metal ions from diffusing outside of pitting, the corrosion products (metal oxide) cover the surface of the pitting, occluding the corrosion cell. As more chloride ions move inside the pitting, the pitting becomes more acidic. It undergoes autocatalytic activities, which increases the dissolution rate, which is high and frequently results in accidents. As a result, substantial research has been done on the stainless-steel pitting mechanism. Pitting corrosion generally happens in places where the passive film's stability is poor, including inclusion and carbide/intermetallic contacts (Wang, et al., 2021). Figure 3 shows the mechanism of pitting corrosion in stainless steel.

Pits on a metal surface do not look good, but if perforation does not happen, they can be innocuous. Pits begin to form at specific locations on a metal surface defect, which may be caused by a breakdown of the coating, mechanical discontinuities, or microstructural phase heterogeneities like secondary phases. In addition to the extended period required for pit formation or pit growth, it is expected that several anodic and cathodic reactions occur at specific locations. Although the anodic and cathodic reaction rates are both slow, the reactions typically move inward and toward gravity (Perez, 2004).

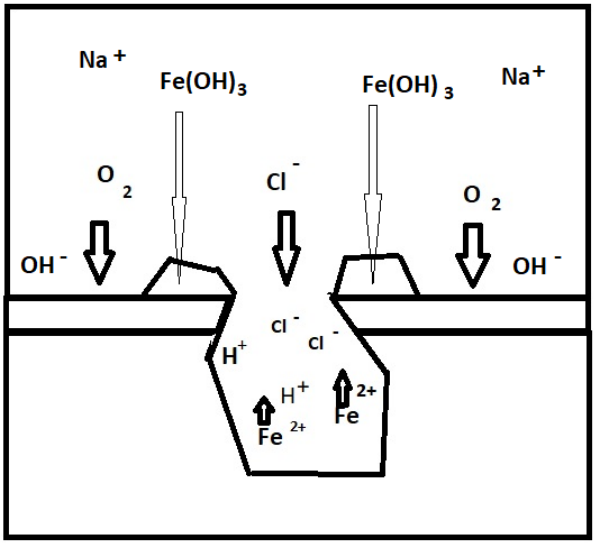

Fig 3. Mechanism of pitting corrosion

The cause of uniform corrosion during the test is due to the oxidation reaction between the hardened S45C steel and the corrosive environment, which in this study, is the HCl solution. In corrosion testing, S45C steel undergoes an oxidation reaction. In this reaction, S45C steel, which has the main composition of iron (Fe), experiences an electron release reaction from Fe2+ to Fe (Hughes et al., 2016). This results in the formation of depressions in the part of S45C steel that has lost Fe atoms due to electron release. Due to this reaction, S45C steel is damaged in the form of an evenly eroded S45C steel surface and leaves stains in the form of rust or deposits. During the test, the reaction between hardened S45C steel and 32% HCl solution also produces iron (II) chloride solution and hydrogen gas.

Numerous studies have been done on the uniform corrosion behavior of stainless steels (austenitic, ferritic, duplex, and ferritic/martensitic) under hot water. According to the literature, a duplex oxide film develops on the surface of stainless steels when they are exposed to high temperature aqueous conditions without a lot of dissolved oxygen. The duplex structure comprises of octahedral magnetite (Fe3O4) crystals on top of a homogenous Cr-rich spinel layer that is placed next to the metal. Similar to what is observed in steam at higher temperatures, the corrosion progresses with growth of the outer oxide, aided by outward diffusion of Fe towards the aqueous interface, and concurrent growth of the inner oxide, via inward diffusion of the oxidizing species. Since oxygen diffuses slowly in spinel-type films, it is assumed that the latter step occurs via transport (Terrani, et al., 2016).

To stop additional uniform corrosion, the low alloy steel surface has a consistent corrosion production film. The density and integrity of the corrosion

production film, which are always impacted by the alloy composition and microstructure, determine the corrosion resistance of low alloy steel. (Wang, et al., 2021). Figure 4 shows the mechanism of uniform corrosion in stainless steel.

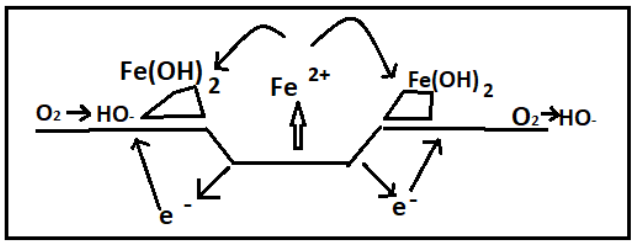

Fig 4. Mechanism of uniform corrosion

Uniform and pitting corrosion prevention can be achieved by selecting 1) suitable materials with uniform microstructure, 2) coating or paint, and 3) inhibitor(s) to delay or eliminate corrosion (Perez, 2004).

Carbon is supersaturated in the martensite of carbon steels in their as-quenched state. It is believed that interstitial carbon has a significant role in martensitic steels' ability to resist pitting and corrosion. Interstitial carbon was also said to increase steel's corrosion resistance in acidic solutions in addition to near-neutral solutions. The presence of interstitial carbon stopped pitting from the beginning and spreading. (Kadowaki, et al., 2017).

4 CONCLUSIONS

The variations of holding time and oil viscosity applied during the hardening process of S45C steel affect the corrosion rate. The increase in holding time causes S45C steel to austenite evenly until it reaches the core. On the other hand, increasing the value of oil viscosity slows the cooling rate, which makes the forming of the martensite structure more difficult. As a result, S45C steel tends to be ductile and soft. In this study, the highest average corrosion rate for S45C steel which was treated with a holding time of 60 minutes and cooled using SAE 0W-20 oil was obtained at 83.2 mm/y. Meanwhile, the highest average corrosion rate for S45C steel treated with a 60-minute holding time and cooled using SAE 20W-50 oil was obtained at 75.4 mm/y. Finally, the types of corrosion were uniform and pitting corrosion.

5. REFERENCES

1. Bardal, Einar. (2004), *Corrosion and Protection*, Springer-Verlag.

2. Berndt, F., & van Bennekom, A. (2001), *Pump shaft failures - a compendium of case studies,* Engineering Failure Analysis, 8, 135–144.

3. Brühl, S. P., Charadia, R., Simison, S., Lamas, D. G., & Cabo, A. (2010), *Corrosion behavior of martensitic and precipitation hardening stainless steels treated by plasma nitriding,* Surface and Coatings Technology, 204(20), 3280–3286. https://doi.org/10.1016/j.surfcoat.2010.03.036

4. Cardoso, P., Santos, A., Rato, R., & Estrela, M. (2017), *Assessment of Pump's Performance in Water Supply Systems - Data Collected from Multiple Case Studies,* European Journal of Sustainable Development, 6(2), 217–226. https://doi.org/10.14207/ejsd.2017.v6n2p217

5. Carlone, P., Palazzo, G. S., & Pasquino, R. (2010), *Finite element analysis of the steel quenching process: Temperature field and solid–solid phase change*, Computers & Mathematics with Applications, 59(1), 585–594. https://doi.org/10.1016/j.camwa.2009.06.006

6. Clover, D., Kinsella, B., Pejcic, B., & de Marco, R. (2005), *The influence of microstructure on the corrosion rate of various carbon steels,* Journal of Applied Electrochemistry, 35(2), 139–149. https://doi.org/10.1007/s10800-004-6207-7

7. Davis, J. (2000), *Corrosion - Understanding the Basics,* ASM International.

8. Hughes, A. E., Mol, J. M., Zheludkevich, M. L., & Buchheit, R. G. (2016), *Fundamentals of Corrosion Kinetics (Vol. 233)*, Springer Netherlands. https://doi.org/10.1007/978-94-017-7540-3

9. Hwang, H., & Park, Y. (2009), *Effects of Heat Treatment on the Phase Ratio and Corrosion Resistance of Duplex Stainless Steel,* Materials Transactions, 50(6), 1548–1552. https://doi.org/10.2320/matertrans.MER2008168

10. Jannifar, A., Ichsan, T. A., Nurdin, H., Mukhtar, F., & Wahyudi, W. (2018). Welding current effect of welded joints of base metal st37 on characteristics: corrosion rate and hardness. *International Conference on Sustainable Energy and Green Technology 2018*, 1–6. https://doi.org/10.1088/1755-1315/268/1/012167

11. Jirarungsatian, C., & Prateepasen, A. (2010), *Pitting and uniform corrosion source recognition using acoustic emission parameters,* Corrosion Science, 52(1), 187–197. https://doi.org/10.1016/j.corsci.2009.09.001

12. Kadowaki, M., Muto, I., Sugawara, Y., Doi, T., Kawano, K., & Hara, Nobuyoshi. (2017). *Pitting Corrosion Resistance of Martensite of AISI 1045 Steel and the Beneficial Role of Interstitial Carbon*. Journal of The Electrochemical Society, 164 (14), C962-C972. http://dx.doi.org/10.1149/2.0541714jes

13. Li, S.-X., & Akid, R. (2013), *Corrosion fatigue life prediction of a steel shaft material in seawater,*

Engineering Failure Analysis, 34, 324–334. https://doi.org/10.1016/j.engfailanal.2013.08.004
14. Li, Z., Zhang, J., Dai, B., & Liu, Y. (2020), *Microstructure and corrosion resistance property of laser transformation hardening pre-hardened AISI P20 plastic die steel*, Optics & Laser Technology, 122, 1–11. https://doi.org/10.1016/j.optlastec.2019.105852
15. Moradi, M., Ghorbani, D., Moghadam, M. K., Kazazi, M., Rouzbahani, F., & Karazi, S. (2019), *Nd:YAG laser hardening of AISI 410 stainless steel: Microstructural evaluation, mechanical properties, and corrosion behavior*, Journal of Alloys and Compounds, 795, 213–222. https://doi.org/10.1016/j.jallcom.2019.05.016
16. Perez, Nestor. (2004) *Electrochemistry and Corrosion Science*, Kluwer Academic Publishers.
17. Terrani, K.A., Pint, B.A., Kim, Y.-J., Unocic, K.A., Yang, Y., Silva, C.M., III, H.M. Meyer, & Rebak, R.B. (2016). *Uniform corrosion of FeCrAl alloys in LWR coolant environments*, Journal of Nuclear Materials, 479, 36-47. https://doi.org/10.1016/j.jnucmat.2016.06.047
18. Vazdirvanidis, A., Pantazopoulos, G., & Rikos, A. (2017). *Corrosion investigation of stainless steel water pump components*. Engineering Failure Analysis, 82, 466–473. https://doi.org/10.1016/j.engfailanal.2016.09.009
19. Wang, Li, Dong, Chao-fang, Man, Cheng, Hu, Ya-bo, Yu, Qiang, & Li, Xiao-gang. (2021), *Effect of microstructure on corrosion behavior of high strength martensite steel—A literature review*, International Journal of Minerals, Metallurgy and Materials, 28(5), 754-773. https://doi.org/10.1007/s12613-020-2242-6
20. Wu, B., Zhang, J., Zhang, L., Pyoun, Y.-S., & Murakami, R. (2014), *Effect of ultrasonic nanocrystal surface modification on surface and fatigue properties of quenching and tempering S45C steel*, Applied Surface Science, 321, 318–330. https://doi.org/10.1016/j.apsusc.2014.09.068
21. Yim, C. D., Kim, Y. M., & You, B. S. (2007), *Effect of Ca Addition on the Corrosion Resistance of Gravity Cast AZ31 Magnesium Alloy*, Materials Transactions, 48(5), 1023–1028. https://doi.org/10.2320/matertrans.48.1023

Received: July 11, 2022 / Accepted: December 15, 2022 / Paper available online: December 20, 2022